

A GENERIC BEACH MORPHODYNAMIC MODEL BY MINIMIZATION PRINCIPLE

R. Dupont^{1,2,3,*}, F. Bouchette^{1,3}, and B. Mohammadi^{2,3}

^{1*} GEOSCIENCES-M, Univ Montpellier, CNRS, Montpellier, France.

² IMAG, Univ Montpellier, CNRS, Montpellier, France.

³ GLADYS, Univ Montpellier, Montpellier, France.

Welcome to my Poster !

Introduction

Morphodynamical models in shallow coastal waters is a challenging topic, especially when trying to reproduce physical phenomena such as sandbar creation. Classic models are generally very complex and highly parameterized; they separately solve the physical equations of hydrodynamics and morphodynamics at a very small scale of the order of second in time and of the wave length in space. The **OptiMorph** model that we have designed proposes a more global approach based on an optimization principle. An example is shown in **Fig. 1** below.

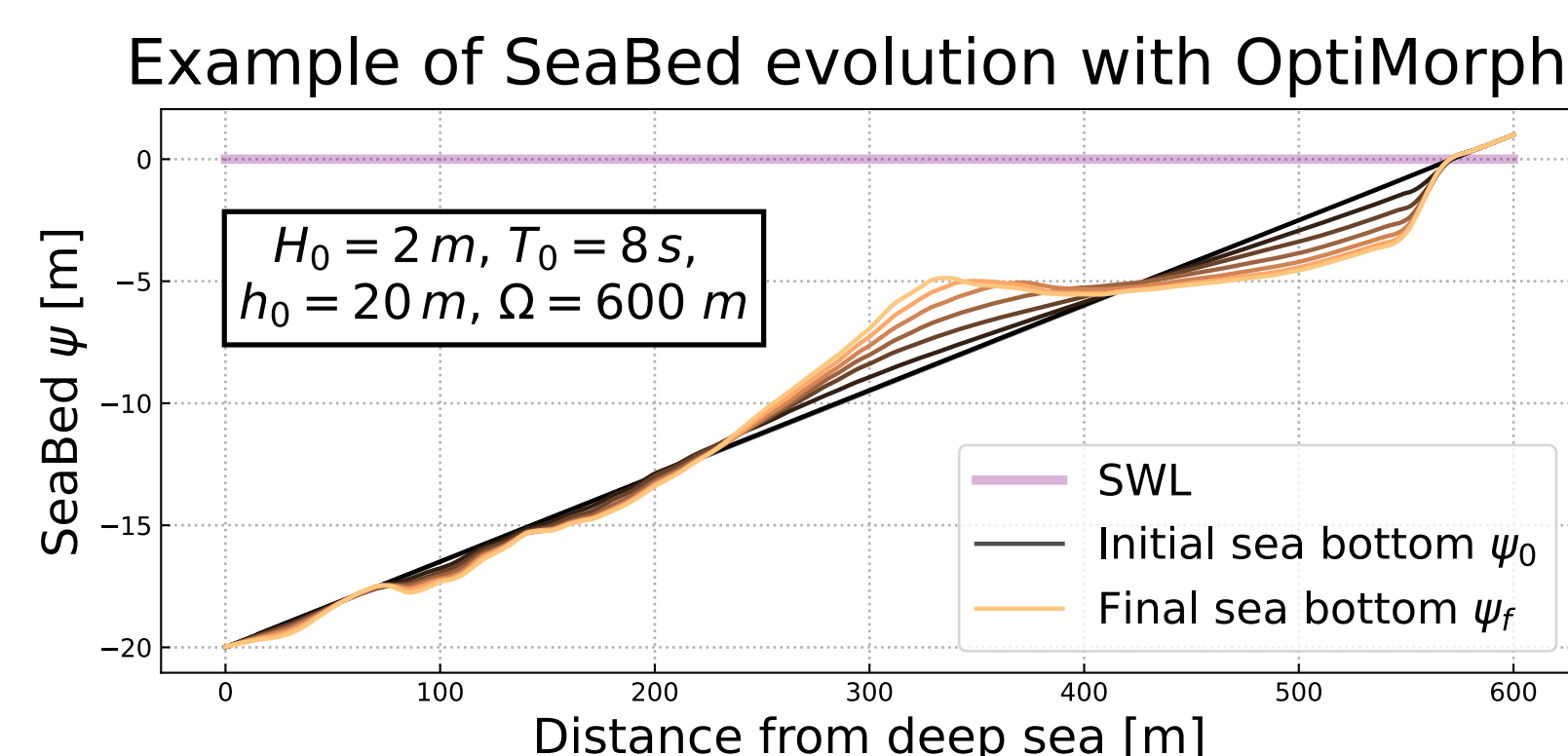


Fig 1. Example of a simulation with OptiMorph coupled to the Shallow-Water model, based on linear Sea Bottom profile.

Models based on the minimization principle rely on the calculation of some derivatives. This can be achieved by heavy methods (automatic differentiation). Our strategy uses the Hadamard derivative to calculate the gradient of any cost function with respect to shape, allowing us to solve the optimization problem at the heart of the model. This strategy has enabled us to create a generic morphodynamic.

Thanks to these advances, we have coupled hydrodynamic models such as Xbeach, SWAN and Shallow-Water and we present simulation results of the flume experiments LIP11D benchmark. Other results presenting the phenomenological aspects of the model are presented on open sea config.

References

- [1] Dupont Ronan, Megan Cook, Frédéric Bouchette, Bijan Mohammadi, and Samuel Meulé (2023). "Sandy beach dynamics by constrained wave energy minimization". In: Ocean Modelling, p. 102197.
- [2] M. Cook. Calcul optimal pour la modélisation de la dynamique naturelle des plages sableuses et la conception d'ouvrages de défense du littoral à faible impact anthropique. Theses, Université Montpellier, Dec. 2021.
- [3] M. Cook, F. Bouchette, B. Mohammadi, L. Sprunck, and N. Frayssé. Optimal Port Design Minimizing Standing Waves with A Posteriori Long Term Shoreline Sustainability Analysis. China Ocean Engineering, 35(6):802–813, Dec. 2021.
- [4] D. Isebe, P. Azerad, F. Bouchette, B. Ivorra, and B. Mohammadi. Shape optimization of geotextile tubes for sandy beach protection. International Journal for Numerical Methods in Engineering, 74(8):1262–1277, May 2008.
- [5] D. Isebe, P. Azerad, B. Mohammadi, and F. Bouchette. Optimal shape design of de-fense structures for minimizing short wave impact. Coastal Engineering, 55(1):35–46, Jan. 2008.
- [6] D. Isebe, P. Azerad, F. Bouchette, and B. Mohammadi. Design of Passive Defense Structures in Coastal Engineering. International Review of Civil Engineering (IRECE), 5(2):75, Mar. 2014.
- [7] B. Mohammadi and F. Bouchette. Extreme scenarios for the evolution of a soft bed interacting with a fluid using the Value at Risk of the bed characteristics. Computers & Fluids, 89:78–87, Jan. 2014.
- [8] B. Mohammadi and A. Bouharguane. Optimal dynamics of soft shapes in shallow waters. Computers & Fluids, 40(1):291–298, Jan. 2011.

Constraints are added to the model to incorporate more physics and to deliver more realistic results.

The first one concerns the sand in the case of an experimental flume. In a flume, the quantity of sand must be constant over time, as given by **Eq 7.a**, contrarily to an open-sea configuration where sand can be transported between the nearshore zone and a domain beyond the closure water depth where sediment is lost definitely for beach morphodynamics. This constraint is illustrated in **Fig 7.a**.

$$\int_{\Omega} \psi(t, x) dx = \int_{\Omega} \psi_0(x) dx \quad (5.a)$$

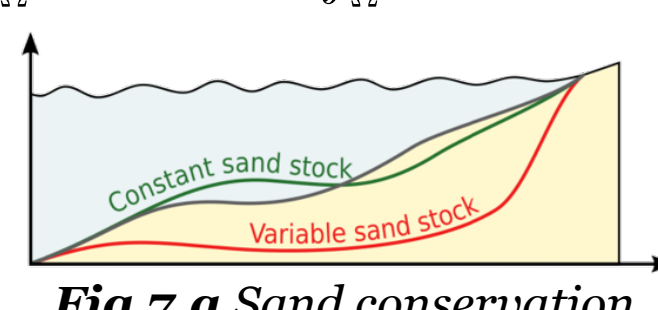


Fig 7.a Sand conservation.

$$\left| \frac{\partial \psi}{\partial x} \right| \leq M_{\text{slope}} \quad (5.b)$$

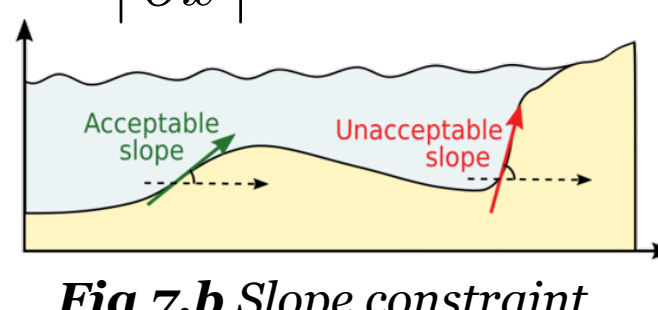


Fig 7.b Slope constraint.

The second concerns the local slope of the bottom. Depending on the composition of the sediment, the bottom slope is bounded by a grain-dependent threshold Mslope. This is conveyed by the constraint on the local bottom slope illustrated by **Fig 7.b**. Mslope, the critical angle is often observed between [0.01, 0.2].

V. Constraints

IV. Morphodynamic

The morphodynamic model is based on the following gradient descent equation (**Eq (4)**),

$$\begin{cases} \psi(t=0) = \psi_0 \\ \psi_t = \Upsilon \Delta d \end{cases} \quad (4)$$

with $d = -\nabla_{\psi} J$ and

$$J(\psi, t) = \frac{1}{16} \rho_w g \int_{\Omega} H^2(\psi, x, t) dx$$

with $d = -\nabla_{\psi} J$ and the other parameters defined in **Tab 2**.

Ψ_t	Evolution of the seabed over time [m/s]
Ψ_0	Initial seabed elevation [m]
Υ	Abrasion of sand [m.s/kg]
Λ	Excitation of the seabed by the waves
Ω	Domain size [m]
ρ_w	Water density [kg/m ³]
g	Gravitational acceleration [m/s ²]
H	Significant wave height [m]

Tab 2. Morphodynamic model parameters.

Gradient descent is constrained (**Eq (4)**), as illustrated in **Fig 6**. Without constraint, the **Eq (4)** would simply be $\psi_t = -\nabla_{\psi} J$. The constraints (represented by α in **Fig 6**) are shown in section V.

I. Forcing

This hydro-morphodynamic model needs a number of forcing parameters (**Tab 1**), divided in 4 parts: numerical, domain, hydrodynamic and morphodynamic. The advantage of this model is that it keep the classical parameters without reference to local sediment transport parameters such as the Shield number.

Physics	Params	Definition
Numerical	Δx	Spatial step [m]
	Δt	Time step [s]
	T_t	Simulation time [s]
Domain	L	Size [m]
	h_0	Offshore depth [m]
	c, M	Tide parameters
Hydro	$H_0(t)$	Offshore water level [m]
	T_0	Wave period [s]
	γ	Breakwater criterion
Morpho	ψ_0	Initial sea bottom
	Υ	Sediment mobility
	β	Maximum slope

Tab 1. Different forcing parameters.

A new parameter Υ , calculated from flux-based morphodynamic is introduced.

II. Hydro-dynamic

Our morphodynamic model can be coupled with any hydrodynamic model. Both spectral and wave-resolved models. However, our numerical model works with an averaged water height as shown in the definition of the cost function J (**Eq (1)**).

Spectral

The spectral models already implemented in the model are SWAN, XBeach and a simple invented Shoaling model.



Wave-resolving models

The classic Shallow-Water model has been implemented. We obtain H as follows:

$$\eta_{RMS} = \sqrt{\frac{1}{k T_0} \int_0^{T_0} \eta^2 dt}, \quad k \in \mathbb{N}$$

The relevance of these models can be seen by comparing them with the LIP1C experiment in **Fig. 3**.

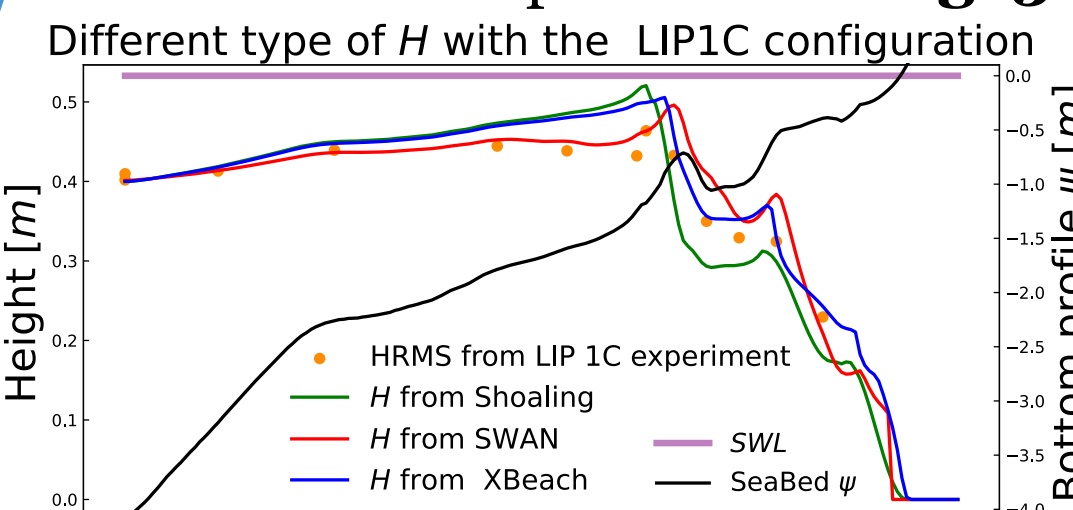


Fig 3. Hydrodynamic results obtained with the Shoaling, SWAN and XBeach models. Bathymetric configurations from the LIP1C channel experiment. Orange points, measured HRMS, black bathymetry, green H from extended shoaling, red H from SWAN, blue H from XBeach.

Hypothesis:

The evolution of the seabed over time is based on the assumption that the seabed evolves in such a way that wave energy is minimized.

The hypothesis is illustrated by the following problem:

$$\min_{\psi} J \quad \text{with} \quad J = \frac{1}{16} \rho_w g \int_{\Omega} H^2 d\Omega \quad (1)$$

with Ψ the sea bottom, H the averaged water height and J the cost-function. This minimization can be observed in the following LIP1C and DynaRev experiments (**Fig 2**) by comparing wave energy at the beginning and end of the experiment.

Comparison of Wave Energy E_H between the beginning and the end of the experience

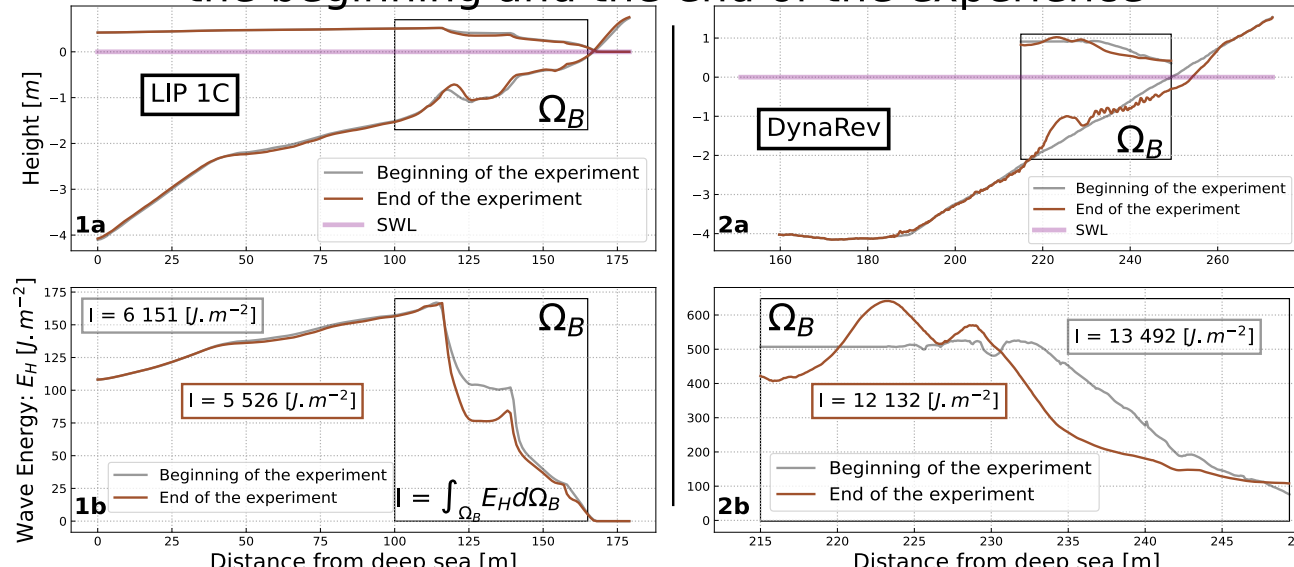


Fig 2. 1) LIP1C experiment with H generated by XBeach. 2) DynaRev experiment with H measured by LIDAR. a) Sea Bottom and averaged water height at the beginning of the experiment (grey). b) Sea Bottom and averaged water height at the end of the experiment (brown). c) Wave energies associated with water heights. The energy is calculated on the grey rectangle.

Solving problem **Eq (1)** involves calculating the gradient of the cost function J with respect to the shape $\nabla_{\psi} J$ (this necessity is described in IV). There are very expensive methods for calculating it (automatic differentiation, etc.). We consider $\nabla_{\psi} J$ in the sense of Hadamard in **Eq (2.a)** and approximated to order 1 in **Eq (2.b)**:

$$\nabla_{\psi} H = \lim_{\varepsilon \rightarrow 0} \frac{H(\psi + \varepsilon n) - H(\psi)}{\varepsilon}, \quad (2.a)$$

$$\approx \lim_{\varepsilon \rightarrow 0} \frac{H(\psi) + \varepsilon \nabla_{\psi} H \cdot n - H(\psi)}{\varepsilon}, \quad (2.b)$$

$$\approx (\nabla_{\psi} H) \cdot n, \quad (2.c)$$

where n is the normal to the shape Ψ . Considering $J=H$, we have **Eq (3)**.

III. Hadamard

$$\nabla_{\psi} H \approx \frac{\partial H}{\partial x} n_x + \frac{\partial H}{\partial y} n_y. \quad (3)$$

Using **Eq (3)** we check on **Fig 5** that the calculation of the numerical gradient is identical to the analytical gradient.

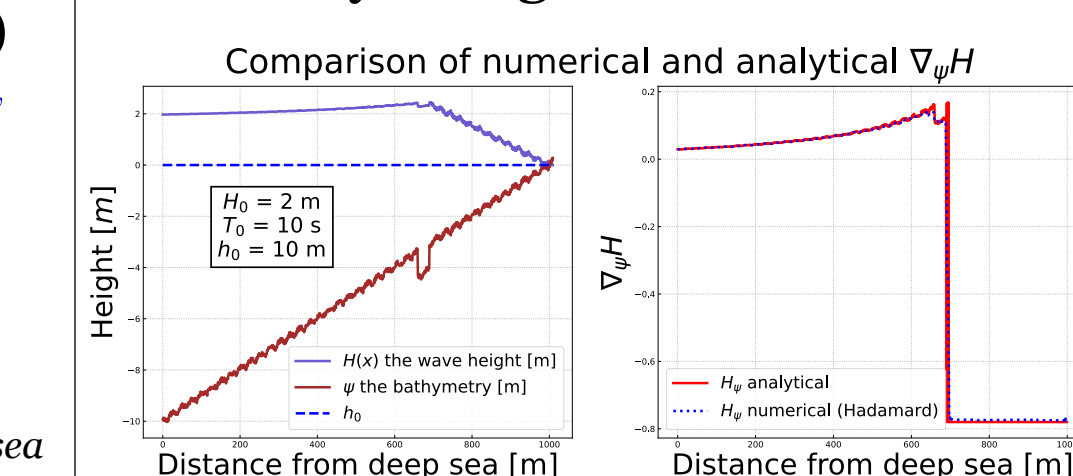


Fig 5. Comparison of numerical and analytical solution of $\nabla_{\psi} H$ using OptiMorph model. In dodgerblue, the wave height H , in brown the bottom profile ψ , in red $\nabla_{\psi} H$ calculated analytically, in blue $\nabla_{\psi} H$ calculated by Hadamard strategy.

Morphodynamic Results: LIP 11D – 1C

The LIP11D - 1C flume experiment is performed with the following parameters: $H_s = 0,6$ m, $T_0 = 5$ s. We run simulations with our OptiMorph model using the Shoaling, SWAN and XBeach hydrodynamic models and we compare them with the experimental results. The results are shown in **Fig 8**.

The results show that the sedimentary bar ($x = 140$ m) appears to be well reproduced by the model. However, our model did not reproduce the behavior of the sediment bar at $x = 110$ m.

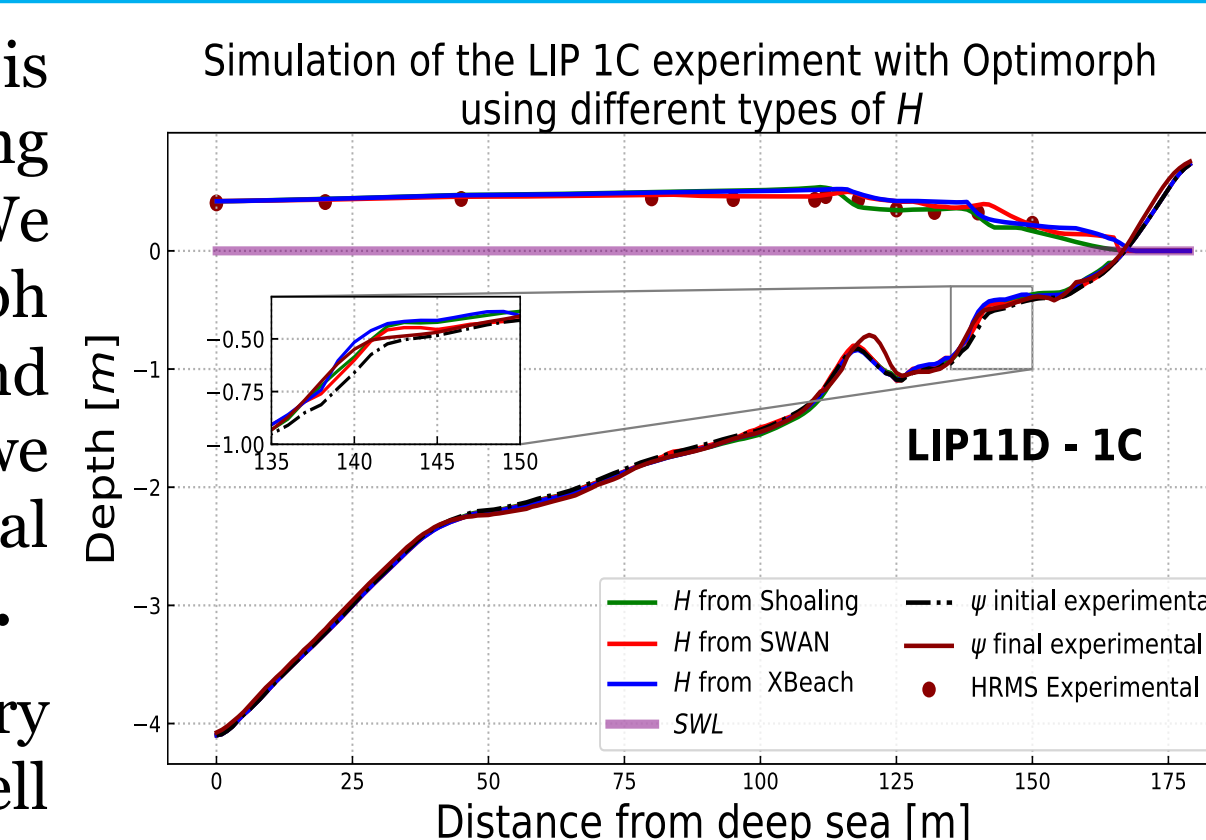


Fig 8. Hydro-Morphodynamic results obtained with LIP-1C experiment and OptiMorph model using Hadamard strategy

Morphodynamic Results: Open-Sea

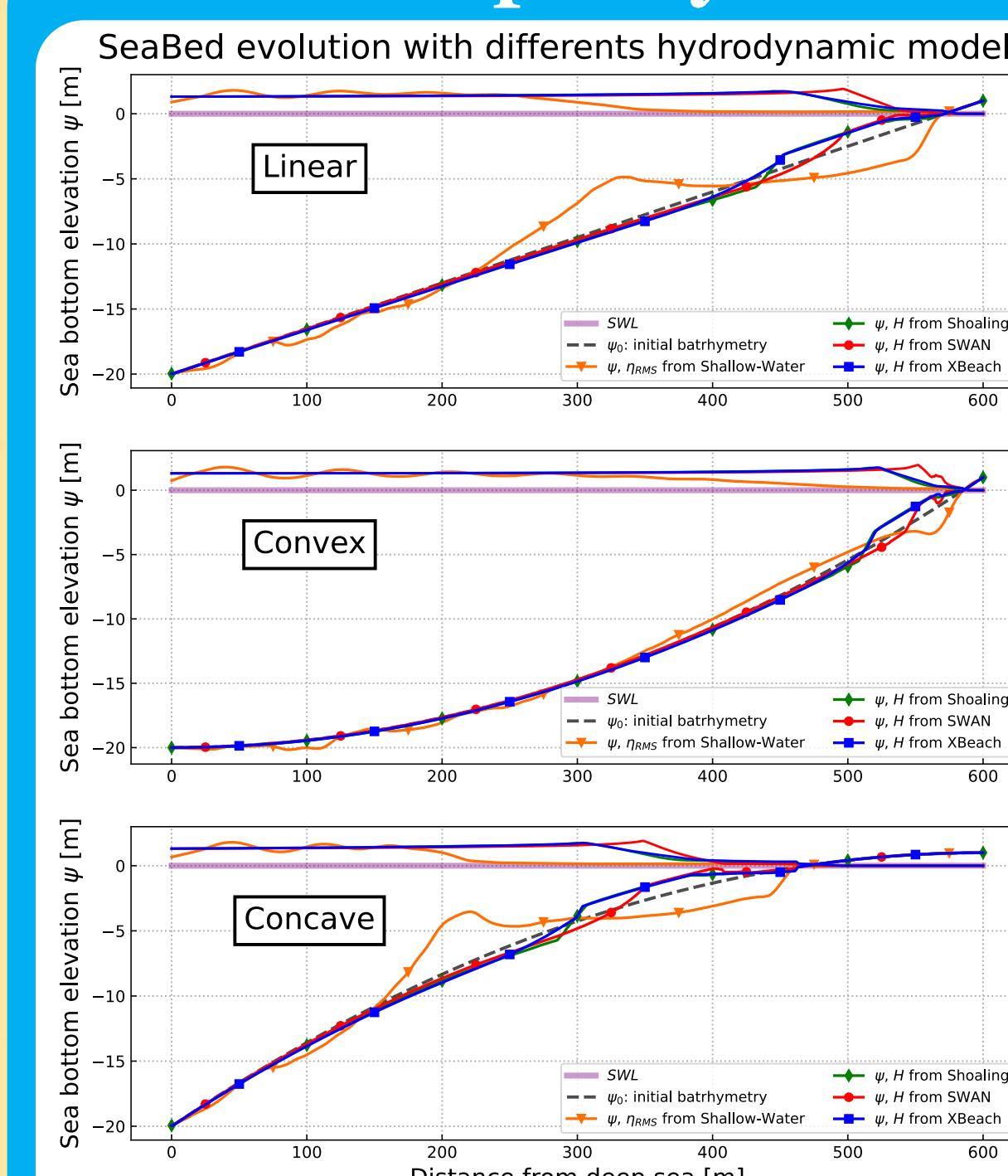


Fig 9. Hydro-Morphodynamic results obtained with Open-Sea configuration and OptiMorph model using Hadamard strategy.

Our model is capable of running simulations in the open sea, as shown in **Fig. 9** on linear, concave and convex sea bottom. These shapes are not directly observable in nature but representative of several typical settings (dissipative, reflexive). For these cases, our model uses the hydrodynamics from SWAN, XBeach, Shoaling and Shallow-Water models. The simulation parameters are as follows: $H_0 = 2$ m, $T_0 = 12$ s, $h_0 = 20$ m, $\Omega = 600$ m.

The results show that the morphodynamic model is able to reproduce the phenomenology of sedimentary evolution of sand beaches with the creation of sedimentary bars.

Discussion

The results show that the model reproduces well the sedimentary bars which are very sensitive to the wave breaking point as shown in **Fig. 10** where the sedimentary bar appears at this point.

The model has the advantage of being fast and low complexity, as shown in **Tab. 3**.

Moreover, it's easily extendable to 2D and can be used to tackle engineering problems such as optimizing the position and shape of coastal defenses.

Simulation with 1000 points	Hydrodynamic	Morphodynamic
Computation time for 1 iteration (s)	Shoaling: 0.013, SWAN: 0.7158, XBeach: 12.243	gradient descent: 0.044
Total computation for with 1000 iterations (mins)	0.966, 1.267, 288.12	0.762

Tab 3. Computation time (with 2.4 GHz computer) with 600 points calculated with different hydrodynamic models.

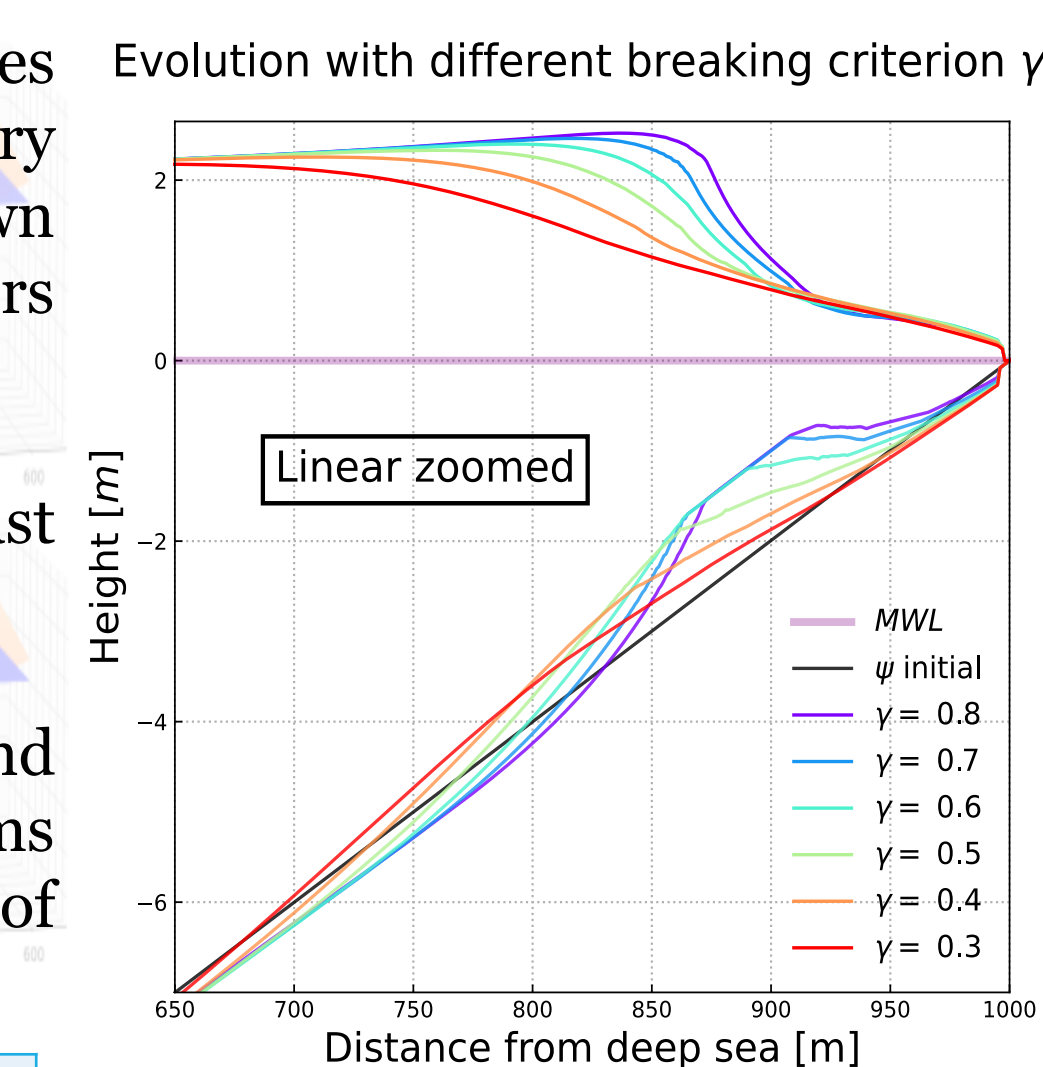


Fig 10. Hydro-morphodynamic results with different breaking criterion γ - Simulation with OptiMorph (Hadamard strategy) using SWAN model - $H_0=2$ m, $T_0=12$ s, $h_0=20$ m.